Identification of an orally active carbazole aminoalcohol derivative with broad-spectrum anti-animal trypanosomiasis activity

Xiao-Li Cai,[a,#] Weisi Wang,[b,#] De-Hua Lai,[a] Xuan Zhang,[a] Junmin Yao,[b] Yingfang Yu,[b] Shizhu Li,[b] Geoff Hide[c], Hongjin Bai[d], Liping Duan,[b,d*] Zhao-Rong Lun[a,c*]

[a]Center for Parasitic Organisms, State Key Laboratory of Biocontrol, School of Life Sciences, Sun Yat-Sen University, Guangzhou 510275, P.R. China

[b]National Institute of Parasitic Diseases, Chinese Center for Disease Control and Prevention, WHO Collaborating Centre for Tropical Diseases, Key Laboratory of Parasitology and Vector Biology of the Chinese Ministry of Health, Shanghai 200025, P.R. China

[c]Ecosystems and Environment Research Centre and Biomedical Research Centre, School of Science, Engineering and Environment, University of Salford, Salford, UK

[d]School of Life Science, Tarim University, Alaer 843300, P.R. China

[#]Both authors contributed equally to this work.

[*]**Corresponding author:** Zhao-Rong Lun, E-mail: lsslzr@mail.sysu.edu.cn; Center for Parasitic Organisms, State Key Laboratory of Biocontrol, School of Life Sciences, Sun Yat-Sen University, Guangzhou 510275, China. Liping Duan, E-mail: duanlp@nipd.chinacdc.cn; National Institute of Parasitic Diseases, Chinese Center for Disease Control and Prevention, WHO Collaborating Centre for Tropical Diseases, Key

Laboratory of Parasitology and Vector Biology of the Chinese Ministry of Health, Shanghai 200025, China.

Abbreviations:

H1401: (3,6-dichloro-9*H*-carbazol-9-yl)-3-(2-methylpiperidin-1-yl) propan-2-ol;

H1402: 1-(3,6-dichloro-9*H*-carbazol-9-yl)-3-(propylamino) propan-2-ol (compound);

H1406: 1-(3,6-dichloro-9*H*-carbazol-9-yl)-3-(4-methylpiperidin-1-yl) propan-2-ol;

H1411: 1-(butylamino)-3-(3,6-dichloro-9*H*-carbazol-9-yl) propan-2-ol (compound);

H1426: 1-(3,6-dichloro-9H-carbazol-9-yl)-3-(octylamino) propan-2-ol (compound)

Abstract

Animal trypanosomiasis, caused by the members of subgenus *Trypanozoon* (*Trypanosoma brucei brucei*, *T. evansi* and *T. equiperdum*), has reduced animal productivity leading to significant negative economic impacts in endemic regions. Due to limited drug discovery and the emergence of drug-resistance over many recent decades, novel and effective compounds against animal trypanosomiasis are urgently required. This study was conducted to evaluate the antitrypanosomal potential of a batch of carbazole aminoalcohol derivatives. Among them, we found that the most effective compound was H1402, which exhibited potent trypanocidal efficacy against the bloodstream-form of *T. b. brucei* (EC_{50} = 0.73 ± 0.05 μM) and presented low cytotoxicity against two mammalian cell lines with CC_{50} > 30 μM. Using a murine model of acute infection, oral administration with H1402 demonstrated a complete clearance of *T. b. brucei* and all the infected mice were cured when they were treated twice daily for 5 days at a dose of 100 mg/kg. Furthermore, parasites were not detected in mice infected with *T. evansi* and *T. equiperdum* (the causative agents of surra and dourine, respectively, in animals) within 30 days following the same regimen with H1402. In addition, H1402 caused severe morphological and ultrastructural destruction to trypanosomes, as well as causing phosphatidylserine externalization, which are suggested to be the most likely cause of cell death. Overall, the present data demonstrated that H1402 could be promising as a rapid, safe and orally active lead compound for the development of new chemotherapeutics for animal trypanosomiasis.

Keywords: antitrypanosomal activity, animal trypanosomiasis, carbazole

aminoalcohols, *T. b. brucei*, *T. equiperdum*, *T. evansi.*

1. Introduction

Three species in the subgenus *Trypanozoon* (*T. brucei*, *T. evansi*, and *T. equiperdum*) are pathogens that cause human African trypanosomiasis (HAT) and animal trypanosomiasis (AT) (Radwanska et al., 2018). Two subspecies of *T. brucei* (i.e., *T. b. gambiense* and *T. b. rhodesiense*) cause HAT in West/Central Africa and East Africa respectively (Bottieau and Clerinx, 2019). However, *T. b. brucei*, *T. evansi*, and *T. equiperdum* are responsible, respectively, for nagana, surra, and dourine in animals. Animal African trypanosomiasis (nagana) caused by *T. b. brucei* is restricted to some African regions due to it is key dependence on the tsetse fly vector for transmission. In contrast, surra and dourine have radiated out of Africa because their causative pathogens, *T. evansi* and *T. equiperdum*, have evolved independence of the tsetse fly for transmission (Lun et al., 2010). *T. evansi* is mechanically transmitted through the bite of many bloodsucking insects, which feed on a wide range of economically important mammals such as water buffalo, cattle, camels, horses and some wild animals, leading to an endemic distribution of surra in Asia, North Africa, Central and South America, as well as some places in Europe (Aregawi et al., 2019; Desquesnes et al., 2013). While *T. equiperdum* infections are mainly restricted to the family Equidae (horses and donkeys) due to a sexual transmission route and also have radiated to a worldwide geographical distribution as animal translocation has occurred (Claes et al., 2005). Animal trypanosomiasis, caused by the three species mentioned above, has resulted in

great economic loss in livestock husbandry as millions of animals die each year due to suffering from anaemia and cachexia after infection. In addition to the huge socio-economic impact, these animal trypanosomes are potentially responsible for causing the spread of trypanosomiasis by unrestricted animal movement. The epidemic regions are threatened by a large reservoir of the parasites in animals, potentially causing outbreaks and reemergence of trypanosomiasis (Radwanska et al., 2018). Although data shows a tremendous overall success in the elimination program for HAT (Gao et al., 2020), the localized prevalence of animal trypanosomes still leaves cause for concern.

The current control of AT mainly relies on chemotherapy in endemic countries. However, in the last few decades, there has been limited available choices of licensed veterinary drugs (diminazene aceturate, homidium bromide/chloride, isometamidium chloride, quinapyramine, suramin sodium and cymelarsan) which are suitable for therapeutic or prophylactic treatment (Giordani et al., 2016). Furthermore, these drugs that are in current use are far from ideal with many drawbacks related to efficacy and toxicity (Matovu et al., 2001). In addition, the emergence of drug-resistant trypanosomes has also been problematic for the successful chemotherapy of AT (Brun et al., 1994; Rayah et al., 1999; Matovu et al., 2001; Zhou et al., 2004; Delespaux et al., 2007). Over the past decades, continuous efforts have been made in researching new trypanocides, but there is still the lack of an ideal drug (Field et al., 2017). In this context, a range of potent, safe and efficacious drugs for the treatment of AT are urgently required.

The carbazole skeleton is a key structure found in many biologically active

compounds. Several studies reported that carbazole derivatives possessed diverse bioactivities, including those that are antibacterial (Rajakumar et al., 2009), antitumor (Gluszynska, 2015), anti-inflammatory (Bandgar et al., 2012) and anti-parasitic, such as found for *Leishmania donovani* (Brendle et al., 2002), *Plasmodium falciparum* (Erath et al., 2015; Molette et al., 2013) and human African trypanosomes (Thomas et al., 2016). In our previous studies, carbazole aminoalcohol derivatives were demonstrated to have broad-spectrum anti-parasitic activities against *Echinococcus* (Wang et al., 2017a), *Plasmodium* and *Schistosoma* (Wang et al., 2017b). Based on these findings, the goal of this study was focused on the potential efficacy of carbazole aminoalcoholes as treatments against the bloodstream-form of *T. b. brucei*. The cytotoxicity profiles of these compounds were also studied using mammalian cell lines. Among them, H1402 was demonstrated to be a promising anti-trypanosomal compound active against *T. b. brucei*, both *in vivo* and *in vitro*, as well as *T. evansi* and *T. equiperdum* infections. Potentially, this could make an important contribution to the identification of novel chemotherapeutic options for these animal diseases. Furthermore, this study presents results of the effects of H1402 on *T. b. brucei* parasites, *in vitro*, demonstrating that it causes severe morphological and ultrastructural alterations and associated phosphatidylserine externalization. However, the detailed mechanism of parasite death caused by H1402 is still unknown.

2. Materials and methods

2.1. Chemicals

The carbazole aminoalcohol compounds were synthesized in-house as previously described (Chen et al., 2018; Wang et al., 2016b) and included 1-(3,6-dichloro-9*H*-carbazol-9-yl)-3-(2-methylpiperidin-1-yl) propan-2-ol (compound H1401, MW: 391 g/mol), 1-(3,6-dichloro-9*H*-carbazol-9-yl)-3-(propylamino) propan-2-ol (compound H1402, MW: 351 g/mol), 1-(3,6-dichloro-9*H*-carbazol-9-yl)-3-(4-methylpiperidin-1-yl) propan-2-ol (compound H1406, MW: 391 g/mol), 1-(butylamino)-3-(3,6-dichloro-9*H*-carbazol-9-yl) propan-2-ol (compound H1411, MW: 365 g/mol), and 1-(3,6-dichloro-9H-carbazol-9-yl)-3-(octylamino) propan-2-ol (compound H1426, MW: 421 g/mol). Diminazene aceturate (PubChem CID:5284544) was purchased from Lanzhou IS Abundant Pharmaceutical Co., Ltd, China.

2.2. Trypanosomes

The bloodstream-form of *T. b. brucei* Lister 427 strain was used in *in vitro* assays. The bloodstream-form of *T. b. brucei* STIB 920, *T. evansi* CPO gz1 and *T. equiperdum* STIB 818 were used in *in vivo* tests.

2.3. Animals

Healthy female Swiss mice (aged 4-6 weeks, 20 ± 2 g) were purchased from the Laboratory Animal Center of Sun Yat-sen University. Animals were housed in ventilated cages with sawdust bedding, and maintained in the animal care facility under controlled conditions (24 ± 2 °C, 45-60% humidity, 12-hour light-dark cycles). The mice were fed with standard rodent feed and water *ad libitum*. Animal care and experimental procedures complied with the Chinese Laboratory Animal Administration

Act (2017). All animal experiments were conducted in accordance with protocols approved by the Laboratory Animal Use and Care Committee of Sun Yat-Sen University under the license no. 31772445.

2.4. *In vitro* trypanocidal assays

An *in vitro* phenotypic screening of our in-house synthesized carbazole aminoalcohol compound library against bloodstream forms of *T. b. brucei* was performed. *T. b. brucei* cells were maintained at a density of below 1×10^6 cells/ml in HMI-9 medium (pH 7.5, Sigma, USA) supplemented with 10% fetal bovine serum (Genetimes ExCell Technology, China) and 1% streptomycin and penicillin (Gibco, USA) at 37 °C in a 5% CO_2 atmosphere (Hirumi and Hirumi, 1989). The compounds were dissolved and diluted in DMSO, resulting in corresponding final concentrations of the stock solution. For compound tests, 0.5 μL of compound (in DMSO) was added to each well (containing 0.5 mL of medium), 0.5 μL of DMSO was added to each control well. For drug screening, parasites in log phase growth ($6\text{-}8 \times 10^5$ cells/ml) were collected and diluted to 1×10^5 cells/ml, and then incubated in the presence of serial concentrations of 0.5, 1.0 and 10.0 μg/ml carbazole aminoalcohol derivatives for primary screening. Using the molecular weight (MW) of each compound, the units in μg/ml were converted into the equivalent μM concentrations as appropriate for each experiment. Eight concentrations ranging from 0.3 μM to 1.4 μM were used for EC_{50} determination of H1402. Diminazene aceturate was taken as the positive control and dissolved in water according to the above method with a final incubation concentration of 0.05 μM. After 24 hours incubation, the number of motile parasites was counted

under a light microscope (LEICA DM500) using a Neubauer chamber (Marienfeld, Germany) and the parasite mortality rate was calculated. The EC_{50} value was calculated with GraphPad Prism software using nonlinear regression.

2.5. Cytotoxicity assays

The cytotoxicity of H1402 against two normal human cell lines was examined using an LDH assay kit (CytoTox 96® Non-Radioactive Cytotoxicity Assay, Promega, USA) according to the manufacturer's protocol. Human embryonic kidney cells (HEK293) and human gastric mucosal epithelial cells (GES1) were seeded into 96-well plates with a density of 5×10^3 cells/well. Cells were plated in triplicate and treated with H1402 at serial concentrations (2.5, 5, 6.25, 7.5, 10, 12.5, 15, 20 and 30 μM) for 24 hours at 37 °C in a 5% CO_2 atmosphere. Control cells received DMSO (final concentration: 0.1%). After incubation, a 50 μl aliquot of each well was transferred to the corresponding well of an assay plate, and 50 μl of the CytoTox 96® reagent was added and incubated for 30 min in the dark at room temperature. After adding 50 μl of stop solution to each well, the assay plate was measured at 490 nm on a microplate reader (Beckman DTX 880). Experiments were repeated twice.

2.6. *In vivo* efficacy studies

Mice were intraperitoneally infected with 1×10^5 parasites of *T. b. brucei, T. evansi,* or *T. equiperdum*. After confirmation of the presence of parasites in the blood (generally 2 days post-infection), the animals were randomly allocated into three groups ($n = 5$ per group): (1) vehicle control, (2) H1402 group and (3) diminazene aceturate group.

H1402 was formulated in 0.5% carboxymethyl cellulose sodium (CMC) solution. Diminazene aceturate was dissolved in double distilled water. Mice in the H1402 group were treated with 0.2 ml of drug suspension (100 mg/kg) twice a day for a period of 5 days by gavage, while the vehicle control mice received an equal volume of 0.5% CMC solution orally. Animals in the diminazene aceturate group were intraperitoneally injected with a single dose of 20 mg/kg (0.2 ml drug solution). All the treatments were initiated at 2 days post-infection. Parasitemia was individually measured by direct microscopic counting of parasites in a drop of tail blood from the infected animal; the low parasitemia in effectively treated mice could not be counted by hemocytometer, so the infection was monitored by observing the blood smears under the microscope. All animals were checked daily for survival from day 0 to day 36. Mice were considered to have been cured if they survived for 30 days after treatment and no parasites were detected on day 36 (the last day of the observation period). All infection experiments were repeated twice.

2.7. Scanning electron microscopy (SEM)

Samples for scanning electron microscopy were prepared as follows, *T. b. brucei* were seeded at 8×10^5 cells/ml in sterile vented cap culture flasks incubation with H1402 at a concentration of 0.7 μM for 2 hours, *T. b. brucei* cells (10^7) were collected and rinsed with phosphate-buffered saline (PBS, pH 7.4). Parasites were allowed to adhere to the coverslips, and then fixed with 2.5% glutaraldehyde for 2 hours at room temperature. After fixation, parasites were washed with PBS three times and dehydrated in a graded alcohol series [30, 50, 70, 90 and 100% (vol/vol)] for 10 minutes each.

Finally, the coverslips were critical-point dried and coated with 8 nm gold nanoparticles (Pt:Pd 80:20, Ted Pella Inc) using a sputter-coater (Cressington Sputter 208 HR, Ted Pella Inc). Images were captured using an electron microscope (S-3400N, Hitachi), with a scanning work distance of 8 mm and a high voltage of 10 kV.

2.8. Transmission electron microscopy (TEM)

T. b. brucei cells were seeded in a sterile culture flask (8×10^5 cells/ml) and incubated with H1402 at a concentration of 0.7 μM for 2 hours at 37 °C. *T. b. brucei* cells (10^7) were collected and rinsed with phosphate-buffered saline (PBS, pH 7.4). Parasites were collected and fixed with 2.5% glutaraldehyde for 2 hours at room temperature. After fixation, parasites were washed 3 times with sodium cacodylate buffer (0.1 M, pH 7.2), and post-fixed with 1% osmium tetroxide solution containing 0.8% potassium ferrocyanide for 1 hour. Cells were subsequently dehydrated in a graded alcohol series [30, 50, 70, 90 and 100% (vol/vol)] for 10 minutes each, and then embedded in araldite. Ultrathin sections were cut on a LEICA EM UC7 ultramicrotome and stained with 1% methanolic uranyl acetate and lead citrate. The sections were visualised using a transmission electron microscope (JEOL JEM-1400Flash).

2.9. Phosphatidylserine externalization assays

Phosphatidylserine exposure was detected by an Annexin V-FITC apoptosis detection kit (Beyotime Biotechnology, China) according to the manufacturer's instructions (de Silva Rodrigues et al., 2016). *T. b. brucei* cells (2×10^5 cells/ml) were treated in the presence or absence of H1402 (0.7 μM) for 2 hours at 37 °C. The collected

cells were washed twice with PBS, and the pellets were resuspended in the binding buffer. Samples were incubated with Annexin V-FITC solution and propidium iodide (PI) solution for 30 minutes at room temperature in the dark. Then 1×10^4 cells from each sample were analyzed using a FC500 flow cytometer (Beckman). DMSO was used as the control.

3. Results

3.1. *In vitro* trypanocidal activity of carbazole aminoalcohol derivatives

Primary screening results revealed that five compounds caused almost 100% fatal damage to trypanosomes at a concentration of 0.5 μg/ml (the units in 0.5 μg/ml could be converted into μM according to the molecular weight of each compound) within 24 hours (Fig 1A-E). Fig 1F shows the EC50 value (0.73 ± 0.05 μM) of H1402 against trypanosomes. The cytotoxic effect of these compounds on the mammalian host cells showed that H1402 did not reduce the viability nor inhibit the proliferation of HEK293 and GES1 cells at a concentration of up to 30 μM (CC_{50} values > 30 μM). Selectivity determination demonstrated that H1402 was the most promising compound with high selectivity indices (CC_{50}/EC_{50}) of > 41.

3.2. *In vivo* efficacy of H1402 against trypanosomes infections

In all tested compounds, H1402 was demonstrated as the most effective one *in vivo*. H1402 was found completely to eliminate trypanosomes (*T. b. brucei*) in mice within 2 days, and ensured 100% animal survival up to 30 days post treatment without

any relapses detected (Fig 2A). Moreover, no parasites were detected in mice inoculated with the blood and tissue homogenate from cured mice, further confirming that these mice were trypanosome free after treatment with H1402 (data not shown). In addition, all the mice showed normal behaviors and no apparent adverse effects were observed throughout the treatments, which indicated that the dosing regimen of H1402 was well tolerated by the animals. The reference drug, diminazene aceturate cured 100% of infected mice. All control mice died between day 4 and day 5 after infection. Animals treated with H1411 were free of parasites for two weeks, but unfortunately a relapse occurred in all mice after two weeks of infection. The other three compounds, H1401, H1406 and H1426, failed to suppress the growth of trypanosomes *in vivo* (data not shown). Additionally, mice infected with *T. evansi* or *T. equiperdum* were also cured by H1402 following the same dosing regimen and method in *T. b. brucei*. All animals survived up to 30 days without relapses (Fig 2B-C).

3.3. H1402 caused severe morphological and ultrastructural damage to *T. b. brucei*

The *in vitro* anti-trypanosome ability of H1402 was further confirmed by the morphological profiles of *T. b. brucei* cells. Unlike the normal morphology in the control trypanosomes, apparent morphological changes including cell membrane damage, rounding of the cells, shortened and twisted parasite bodies, were observed in the *T. b. brucei* incubated with H1402 (Fig 3). Specifically, H1402 caused fatal damage to parasites, culminating in the rupture of the plasma membrane (Fig 3C). TEM was performed to analyze the effects of H1402 on the ultrastructure of *T. b. brucei* cells (Fig 4). Control parasites showed a clear nucleus, intact nuclear membrane, homogeneous

cytoplasm and normal organelle structures (Fig 4A-B). In contrast, exposure to H1402 resulted in devastating damage to the parasite cells (Fig 4C-F). The most conspicuous features of the ultrastructural alterations were the formation of numerous atypical vacuole-like structures in the cytoplasm and the cell membrane appeared to have a much more ill-defined shape; we also observed dissolved nuclear membranes (Fig 4C) and dilated kinetoplasts (Fig 4E-F).

3.4. H1402 induced obvious phosphatidylserine externalization in *T. b. brucei*

Furthermore, phosphatidylserine externalization was observed in H1402 treated trypanosomes (Fig 5). The proportion of the parasites labelled with PI (45.7%) or both PI and FITC (48.1%) increased significantly in comparison to the untreated cells. Annexin V-FITC/PI analysis revealed that 0.1% of cells were labelled in the untreated group. After exposure for 2 hours, H1402 induced a very high proportion of the parasites to undergo obvious phosphatidylserine externalization. Although this could explain the lethal mechanism of H1402 on the trypanosomes, further investigation is necessary to fully understand the process.

4. Discussion

Following much emphasis on human trypanosomiasis, neglecting the widespread animal trypanosomiasis (AT) has resulted in a potential area of concern. Currently, there is only a limited set of available drugs for animal trypanosomes and these have been used for many decades with subsequent drug resistance being reported (Brun et al., 1994; Rayah et al., 1999). Therefore, there is an urgent requirement for the development

301 of new compounds which can be more easily administered, less toxic, more effective
302 against AT and can circumvent drug resistance.

303 In this study, five carbazole aminoalcohol derivatives were identified to have
304 excellent effects against *Trypanosoma brucei brucei in vitro*, but only H1402 was found
305 effectively to eliminate animal trypanosomes including *T. b. brucei*, *T. evansi* and *T.*
306 *equiperdum in vivo.* Although the effective oral administration dosage of H1402 was
307 higher than the use of current trypanocides (Giordani et al., 2016), it generally did not
308 cause significant adverse effects or toxicity to mice with a long treatment regimen (30
309 days) and were well-tolerated in the animal model (Wang et al., 2017a). The difference
310 in dosage used for the treatment of animal trypanosomes between H1402 and the
311 commercial drugs might be caused by a difference in the mode of administration. In
312 fact, previous studies demonstrated that such carbazole aminoalcohol derivatives
313 displayed only moderate cytotoxicity to rat L6 cells (Wang et al., 2016a). Based on their
314 effectiveness and low toxicity, these carbazole aminoalcohol derivatives show great
315 potential as future drugs. Of course, more research needs to be carried out on these
316 derivatives to determine the mode of action of these compounds against trypanosomes
317 and other parasites.

318 The lethal and rapid damage to trypanosomes caused by H1402 was clearly
319 revealed by SEM/TEM analysis and phosphatidylserine externalization, and these
320 results may indicate a direct killing effect of H1402 with high efficiency on
321 trypanosomes. Such fatal morphological and ultrastructural damages were also
322 observed in *Echinococcus granulosus* treated with H1402 (Wang et al., 2017a).

However, the mechanism of action of this compound against parasites is not known. Some results indicated that the carbazole-derived compounds might block mitosis of trypanosomes (Thomas et al., 2016), but we did not investigate this in our study, since our work was focused on the effect of these compounds on eliminating trypanosomes. In fact, various mechanisms of action of these compounds have been suggested to act in a broad range of parasites including inhibition of the formation of β-hematin in *Plasmodium falciparum* and *Schistosoma japonicum* (Wang et al., 2017b) or targeting the *P. falciparum* Hsp90 (Wang et al., 2016a). Although the exact mechanism of these compounds against parasites are not well understood, the broad spectrum antiparasitic activities of these derivatives have provided a promising chemical scaffold for developing new anti-parasitic medicines.

Additionally, our results generate suggestions for further optimization of these carbazole-derived compounds. The five carbazole aminoalcohol derivatives identified in our study contain the dichlorinated carbazole acting as the privileged core and have a slightly different alkylamine tail. An extensive structure-activity relationship (SAR) study has showed that similar modifications at the 3- and/or 6-positions and the N-alkyl of the carbazole aminoalcohol core could lead to the identification of new derivatives with an excellent *in vitro* potency against several drug resistant strains of *P. falciparum* (K1, NF54, D6, W2, TM91C235, 7G8, and VIS) (Molette et al., 2013). Interestingly, of the five highly similar carbazole aminoalcohol compounds with similar effects *in vitro*, only H1402 showed effectiveness against trypanosomes *in vivo* via oral administration. Therefore, we speculate that a short aliphatic chain at alkylamine tail

may contribute to an improved bioavailability of H1402 *in vivo*. Of course, more detailed SAR studies are required to establish this.

In conclusion, our data have demonstrated that the carbazole aminoalcohol compound, H1402, is a potent, safe and orally bioavailable anti-trypanosomal agent for animals, which could be used as a promising lead compound for drug development against animal trypanosomiasis. Given the broad-spectrum activity and the excellent oral bioavailability of this class of compounds, application to the human trypanosomes, *T. b. gambiense* and *T. b. rhodesiense*, is worth considering to combat potential recrudescence of sleeping sickness in a post-elimination Africa.

Competing interests

The authors declare that they have no known competing financial interests or personal relationships which have, or could be perceived to have, influenced the work reported in this article.

Acknowledgments

We thank Professor Keith Gull of Oxford University for providing *T. b. brucei* Lister 427 strain. This work was supported by grants from the National Natural Science Foundation of China (#31720103918 to Z.-R.L. and #U1803282 to W.W.), and the Open Project of Xinjiang Production & Construction Crops Key Laboratory of Protection and Utilization of Biological Resources in Tarim Basin (BRZD1503).

References

Aregawi, W.G., Agga, G.E., Abdi, R.D., Buscher, P., 2019. Systematic review and meta-analysis on the global distribution, host range, and prevalence of *Trypanosoma evansi*. Parasit Vectors 12, 67. https://doi.org/10.1186/s13071-019-3311-4

Bandgar, B.P., Adsul, L.K., Chavan, H.V., Jalde, S.S., Shringare, S.N., Shaikh, R., Meshram, R.J., Gacche, R.N., Masand, V., 2012. Synthesis, biological evaluation, and docking studies of 3-(substituted)-aryl-5-(9-methyl-3 carbazole)-1H-2-pyrazolines as potent anti-inflammatory and antioxidant agents. Bioorg Med. Chem. Lett. 22, 5839-5844. https://doi.org/10.1016/j.bmcl.2012.07.080

Bottieau, E., Clerinx, J., 2019. Human African Trypanosomiasis: progress and stagnation. Infect Dis Clin North Am. 33, 61-77. https://doi.org/10.1016/j.idc.2018.10.003

Brendle, J.J., Outlaw, A., Kumar, A., Boykin, D.W., Patrick, D.A., Tidwell, R.R., Werbovetz, K.A., 2002. Antileishmanial activities of several classes of aromatic dications. Antimicrob Agents Chemother. 46, 797-807. https://doi.org/10.1128/aac.46.3.797-807.2002

Brun, R., Lun, Z.-R., 1994. Drug sensitivity of Chinese *Trypanosoma evansi* and *Trypanosoma equiperdum* isolates. Vet. Parasitol. 52, 37-46. https://doi.org/10.1016/0304-4017(94)90033-7

Chen, Z., Yang, T., Wang, W., Yao, J., Han, S., Tao, Y., Wang, R., Duan, L., 2018. Synthesis and biological evaluation of carbazole aminoalcohols as antitumor

agents. ChemistrySelect, 3, 12630-12638. https://doi.org/10.1002/slct.201803029

Claes, F., Buscher, P., Touratier, L., Goddeeris, B.M., 2005. *Trypanosoma equiperdum*: master of disguise or historical mistake? Trends Parasitol. 21, 316321. https://doi.org/10.1016/j.pt.2005.05.010

Delespaux, V., de Koning, H.P., 2007. Drugs and drug resistance in African trypanosomiasis. Drug Resist Updat. 10, 30-50. https://doi.org/10.1016/j.drup.2007.02.004

de Silva Rodrigues, J.H., Stein, J., Strauss, M., Rivarola, H.W., Ueda-Nakamura, T., Nakamura, C.V., Duszenko, M., 2016. Clomipramine kills *Trypanosoma brucei* by apoptosis. Int. J. Med. Microbiol. 306, 196-205. https://doi.org/10.1016/j.ijmm.2016.03.009

Desquesnes, M., Holzmuller, P., Lai, D.H., Dargantes, A., Lun, Z.R., Jittaplapong, S., 2013. *Trypanosoma evansi* and surra: a review and perspectives on origin, history, distribution, taxonomy, morphology, hosts, and pathogenic effects. Biomed. Res. Int. 2013, 194176. https://doi.org/10.1155/2013/194176

Erath, J., Gallego-Delgado, J., Xu, W., Andriani, G., Tanghe, S., Gurova, K.V., Gudkov, A., Purmal, A., Rydkina, E., Rodriguez, A., 2015. Small-molecule xenomycins inhibit all stages of the *Plasmodium* life cycle. Antimicrob Agents Chemother 59, 1427-1434. https://doi.org/10.1128/AAC.04704-14

Field, M.C., Horn, D., Fairlamb, A.H., Ferguson, M.A., Gray, D.W., Read, K.D., De Rycker, M., Torrie, L.S., Wyatt, P.G., Wyllie, S., Gilbert, I.H., 2017. Anti-trypanosomatid drug discovery: an ongoing challenge and a continuing need. Nat.

Rev. Microbiol. 15, 217-231. https://doi.org/10.1038/nrmicro.2016.193

Gao, J.M., Qian, Z.Y., Hide, G., Lai, D.H., Lun, Z.R., Wu, Z.D., 2020. Human African trypanosomiasis: the current situation in endemic regions and the risks for non-endemic regions from imported cases. Parasitology, 1-10. https://doi.org/10.1017/S0031182020000645

Giordani, F., Morrison, L.J., Rowan, T.G., DeKoning, H.P., Barrett, M.P., 2016. The animal trypanosomiases and their chemotherapy: a review. Parasitol. 143, 1862-1889. https://doi.org/10.1017/S0031182016001268

Gluszynska, A., 2015. Biological potential of carbazole derivatives. Eur. J. Med. Chem. 94, 405-426. https://doi.org/10.1016/j.ejmech.2015.02.059

Hirumi, H., Hirumi, K., 1989. Continuous cultivation of *Trypanosoma brucei* blood stream forms in a medium containing a low concentration of serum protein without feeder cell layers. J. Parasitol. 75, 985-989

Lun, Z.R., Lai, D.H., Li, F.J., Lukes, J., Ayala, F.J., 2010. *Trypanosoma brucei*: two steps to spread out from Africa. Trends Parasitol. 26, 424-427. https://doi.org/10.1016/j.pt.2010.05.007

Matovu, E., Seebeck, T., Enyaru, J.C.K., Kaminsky R., 2001. Drug resistance in *Trypanosoma brucei* spp., the causative agents of sleeping sickness in man and nagana in cattle. Microbes Infect. 3(9), 763-70. https://doi.org/10.1016/S1286-4579(01)01432-0

Molette, J., Routier, J., Abla, N., Besson, D., Bombrun, A., Brun, R., Burt, H., Georgi, K., Kaiser, M., Nwaka, S., Muzerelle, M., Scheer, A., 2013. Identification and

433 optimization of an aminoalcohol-carbazole series with antimalarial properties.
434 ACS Med Chem Lett. 4, 1037-1041. https://doi.org/10.1021/ml400015f
435 Radwanska, M., Vereecke, N., Deleeuw, V., Pinto, J., Magez, S., 2018. Salivarian
436 trypanosomosis: a review of parasites involved, their global distribution and their
437 interaction with the innate and adaptive mammalian host immune system. Front
438 Immunol. 9, 2253. https://doi.org/10.3389/fimmu.2018.02253
439 Rajakumar, P., Sekar, K., Shanmugaiah, V., Mathivanan, N., 2009. Synthesis of novel
440 carbazole based macrocyclic amides as potential antimicrobial agents. Eur. J. Med.
441 Chem. 44, 3040-3045. https://doi.org/10.1016/j.ejmech.2008.07.031
442 Rayah, I.E.E., Kaminsky, R., Schmid, C., Malik, K.H.E., 1999. Drug resistance in
443 Sudanese *Trypanosoma evansi*. Vet. Parasitol. 80, 281-287.
444 https://doi.org/10.1016/s0304-4017(98)00221-0
445 Thomas, S.M., Purmal, A., Pollastri, M., Mensa-Wilmot, K., 2016. Discovery of a
446 carbazole-derived lead drug for human African trypanosomiasis. Sci. Rep. 6,
447 32083. https://doi.org/10.1038/srep32083
448 Wang, T., Maser, P., Picard, D., 2016a. Inhibition of *Plasmodium falciparum* Hsp90
449 contributes to the antimalarial activities of aminoalcohol-carbazoles. J Med Chem.
450 59, 6344-6352. https://doi.org/10.1021/acs.jmedchem.6b00591
451 Wang, W., Li, J., Yao, J., Wang, T., Li, S., Zheng, X., Duan, L., Zhang, W., 2017a. *In*
452 *vitro* and *in vivo* efficacies of novel carbazole aminoalcohols in the treatment of
453 cystic echinococcosis. J. Antimicrob. Chemother. 72, 3122-3130.
454 https://doi.org/10.1093/jac/dkx250

Wang, W., Li, Q., Wei, Y., Xue, J., Sun, X., Yu, Y., Chen, Z., Li, S., Duan, L., 2017b. Novel carbazole aminoalcohols as inhibitors of beta-hematin formation: antiplasmodial and antischistosomal activities. Int. J. Parasitol. Drugs Drug Resist. 7, 191-199. https://doi.org/10.1016/j.ijpddr.2017.03.007

Wang, W., Sun, X., Sun, D., Li, S., Yu, Y., Yang, T., Yao, J., Chen, Z., Duan, L., 2016b. Carbazole aminoalcohols induce antiproliferation and apoptosis of human tumor cells by inhibiting topoisomerase I. Chem. Med. Chem. 11, 2675-2681. https://doi.org/10.1002/cmdc.201600391

Zhou, J., Shen, J., Liao, D., Zhou, Y., Lin, J., 2004. Resistance to drug by different isolates *Trypanosoma evansi* in China. Acta Trop. 90, 271-275. https://doi.org/10.1016/j.actatropica.2004.02.002

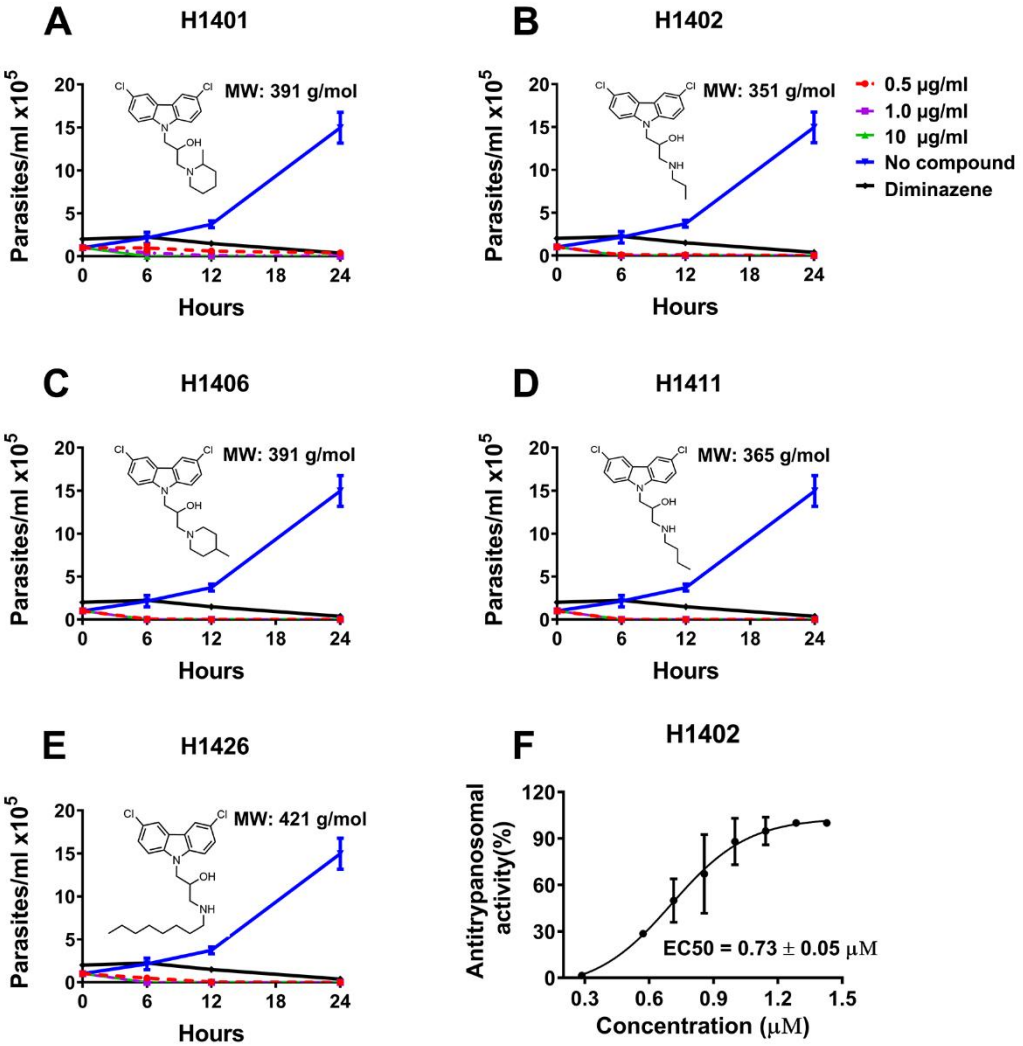

Fig 1. *In vitro* trypanocidal activities of carbazole aminoalcohols. (A-E) Chemical structures and antitrypanosomal activities of five hit compounds; Diminazene aceturate was used as a control with incubation concentration of 0.05 μM. (F) The growth inhibition curve of *T. b. brucei* cells incubated with H1402 at the indicated concentrations for 24 hours.

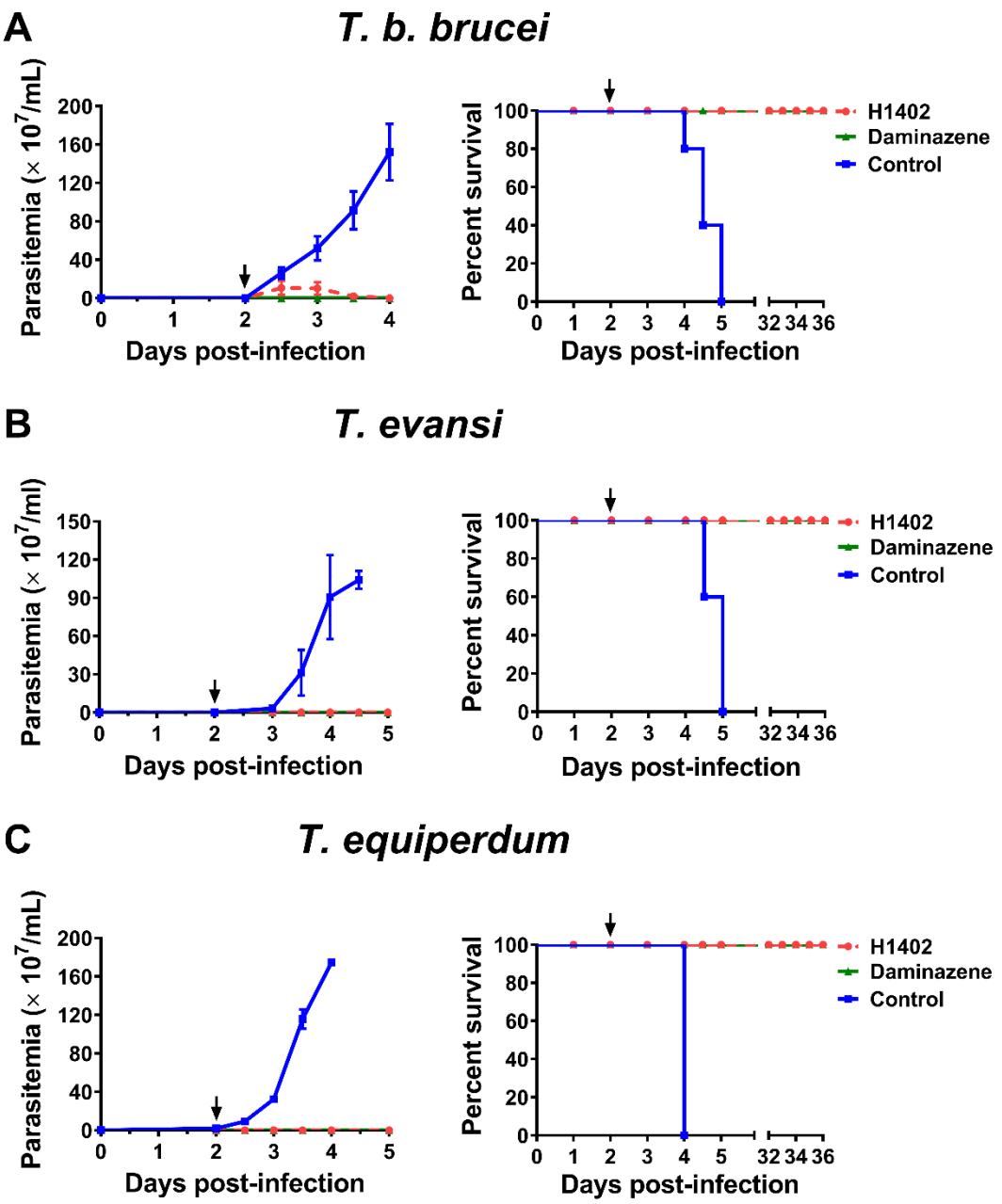

Fig 2. *In vivo* efficacy of H1402 against *T. b. brucei* (A), *T. evansi* (B) and *T. equiperdum* (C) infections. Mice ($n = 5$) were infected with 1×10^5 bloodstream forms of each strain at day 0. Treatment with H1402 (100 mg/kg, p.o., b.i.d. × 5 days) or diminazene aceturate (20 mg/kg, i.p., single dose) was initiated at day 2 (indicated by black arrows). The control group received 0.5% CMC. Parasitemia levels and survival rate curves are shown. b. i. d., twice a day; p.o., per os; i.p., intraperitoneal.

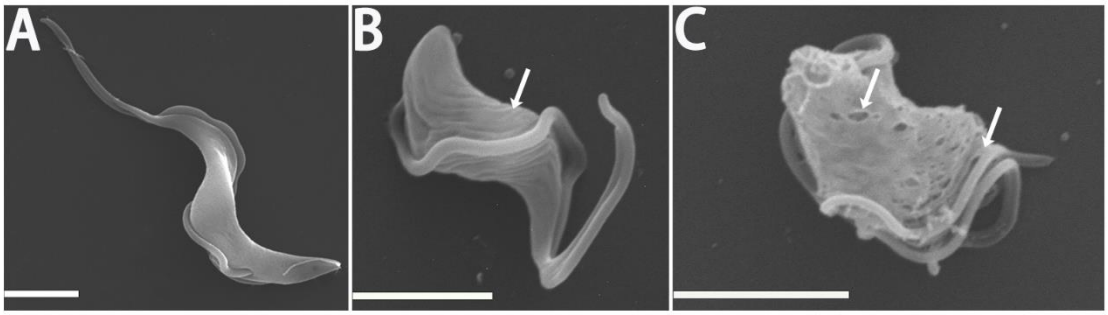

Fig 3. Morphological status of *T. b. brucei* cells treated with H1402 for 2 hours and examined by SEM. (A) Morphology of *T. b. brucei* without H1402 treatment; (B-C) morphology of *T. b. brucei* treated with H1402 (0.7 μM) for 2 hours. Cell membrane damage, spiral, twisted and round cell shapes with the flagella encompassing the cell periphery (white arrows) were found. Bars = 2 μM.

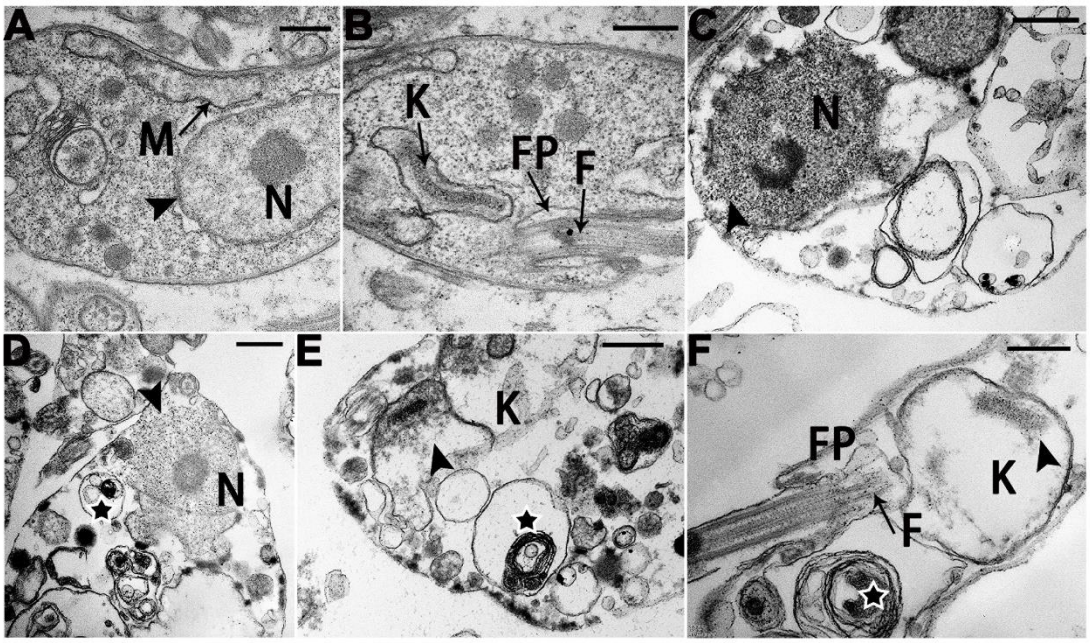

Fig 4. Ultrastructural alterations in *T. b. brucei* cells treated with H1402 and examined by TEM. (A-B) Control parasites; (C-F) H1402 (0.7 μM)-treated parasites showed ill-defined cell shapes and an increase of vacuole-like structures (black stars); (C-D) structures suggestive of dissolved nuclear membranes (black short arrow) and (E-F) dilated kinetoplasts were observed (black short arrow). N, nuclei; K, kinetoplast; M, mitochondrial; F, flagellum; FP, flagella pocket. Bars = 0.5 μM.

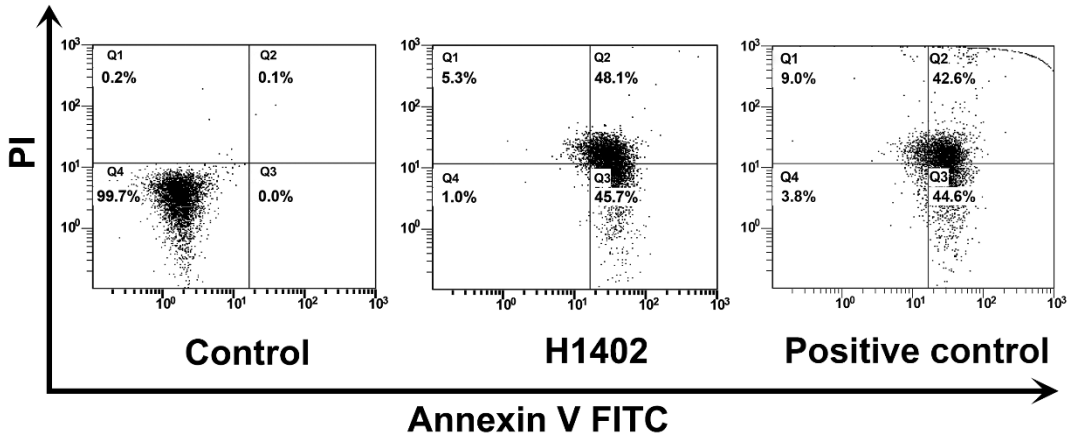

Fig 5. Flow cytometry analysis of H1402-induced phosphatidylserine externalization. Bloodstream forms of *T. b. brucei* were incubated with H1402 (0.7 μM) for 2 hours, and double stained with Annexin V-FITC and PI.

535